THE JOURNAL OF PHYSICAL CHEMISTRY B

Article

pubs.acs.org/JPCB

Molecular Dynamics Simulations and Structural Descriptors of Radioisotope Glass Vectors for In Situ Radiotherapy

Jamieson K. Christie and Antonio Tilocca*

Department of Chemistry and Thomas Young Centre, University College London, 20 Gordon Street, London WC1H 0AJ, U.K.

Supporting Information

ABSTRACT: The low solubility (high durability) of yttrium aluminosilicate (YAS) glass is one of its most important properties for use in in situ radiotherapy. Simple parameters, such as silica or yttria content or network connectivity, are not sufficient to rationalize the dependence of the solubility on the glass composition observed experimentally. We performed classical molecular dynamics (MD) simulations of eight different YAS glasses of known solubility and analyzed the MD trajectories to identify specific structural features that are correlated and can be used to predict the solubility. We show that the (Si−)O−Si coordination number CN_{SiOSi}, the yttrium−yttrium clustering ratio R_{YY}, and the number of intratetrahedral O−Si−O bonds per yttrium atom N_{intra} can be combined into a single structural descriptor $s = f(CN_{SiOSi},R_{YY},N_{intra})$ with a high correlation with the solubility. The parameter s can thus be calculated from MD simulations and used to predict the solubility of YAS compositions, allowing one to adjust them to the range required by radiotherapy applications. For instance, its trend shows that high-silica- and low-yttria-content YAS glasses should be sufficiently durable for the radiotherapy application, although additional clinical considerations may set a lower limit to the yttria content.

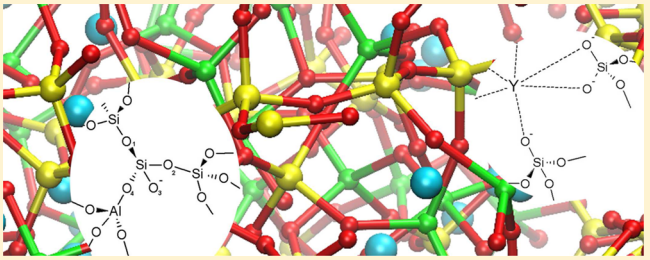

INTRODUCTION

Yttrium aluminosilicate (YAS) glass is used in in situ radiotherapy.[1,2] Conventional radiotherapy irradiates tumors from a radiation source external to the body. The need to avoid damage to the healthy tissue surrounding the tumor limits the maximum dosage of radiation that can be applied. By contrast, in situ radiotherapy uses a radiation source inside the body to irradiate the tumor. YAS glass microspheres are used as the vector for the ^{90}Y radioisotope; following neutron activation, a solution of YAS glass microspheres is injected directly into the tumor or into the blood vessels surrounding it. The tumor is then irradiated from within, reducing the damage to healthy surrounding tissue while increasing the local dosage of radiation. This substantially improves the efficacy of the therapy: the five-year survival rate following this treatment for hepatocellular carcinoma is 46%,[3] compared with typical rates of <7% for conventional radiotherapy.[4]

A key requirement for successful application of this therapy is that the YAS glass used has high durability. The glass must release as little radioactive ^{90}Y into the bloodstream as possible; any ^{90}Y so released would travel throughout the body, irradiating the patient with potentially fatal results. Since the half-life of ^{90}Y is 2.7 days,[5] this means that the glass must be durable for a period of several weeks. Erbe and Day[6] measured the weight loss when eight different compositions of YAS glass were placed in water and acidic environments, and the most durable of these compositions (17.0 mol % Y_2O_3, 18.9 mol % Al_2O_3, and 64.1 mol % SiO_2) is now the composition used in the treatment. They observed a range of composition-dependent weight losses covering more than a factor of 4 in magnitude. Understanding the way in which the glass composition controls its dissolution is the key to optimizing the application of YAS and related materials for radiotherapy.

Computer simulations allow us to investigate the properties of glasses at the atomistic level,[7−10] revealing nonobvious relationships between composition, structure, dissolution behavior, and biological activity in a physiological environment.[11−14] Understanding these relationships also helps to identify suitable directions for optimization of the glass for specific applications. Because most of the structural features that affect durability (e.g., network connectivity and ion clustering[15]) involve the medium-range structure (i.e., the structure on a length scale of about 2−10 nearest-neighbor distances), classical MD simulations with a suitable empirical force field[13] are needed, to study models large enough to capture reliable statistics on the medium-range structure of the glass.

In this paper, we perform MD simulations of the YAS glass compositions previously manufactured by Erbe and Day,[6] and from analysis of the MD trajectories, we devise a structural descriptor[16−18] for YAS glasses, that is, a single parameter that correlates well with the experimentally measured solubilities.[6] This descriptor combines several structural properties extracted from the simulations, and its change with composition allows us

Received: May 1, 2012
Revised: September 12, 2012
Published: September 14, 2012

ACS Publications © 2012 American Chemical Society

to rationalize the experimentally observed composition-dependent changes in solubility. We discuss the possibilities of further optimization of YAS glasses for in situ radiotherapy through MD simulations and the new structural descriptor.

METHODS

As in other related simulation studies,[11,13,19] our general approach involves modeling the bulk glass and analyzing specific bulk structural features linked to, and thus able to rationalize, their (experimental) dissolution behavior. A key reference for the latter is the work of Erbe and Day,[6] who measured the weight loss in water and acidic media of eight different compositions of YAS glass. The solubility of the YAS glasses in water, which best corresponds to the physiological environment, is rather small, and so the data have proportionally large experimental errors. Our analysis, therefore, considered the solubility data at pH = 2, which follow a similar trend, and have a larger absolute value, substantially reducing the relative size of the experimental error. Table 1 lists

Table 1. Compositions, Simulated Densities, and Experimentally Measured Weight Loss per Surface Area of YAS Glass Compositions after 6 Weeks at pH = 2[6]

	mol %				
composition	Y_2O_3	Al_2O_3	SiO_2	simulated dens. (g/cm^3)	wt loss (mg/cm^2)
YAS-10	15.6	34.4	50.0	3.11	14.5
YAS-4	17.0	18.9	64.1	3.20	3.8
YAS-6	19.0	25.0	56.0	3.32	10.6
YAS-3	24.1	21.4	54.5	3.64	12.8
YAS-9	27.4	16.5	56.1	3.84	15.3
YAS-2	28.5	22.9	48.6	3.91	17.9
YAS-11	30.0	15.0	55.0	4.00	18.0
YAS-12	30.0	20.0	50.0	4.00	18.2

the compositions and their weight loss per unit area (which we take as a measure of the solubility) after immersion for 6 weeks in a solution with pH = 2. The compositions are listed in order of increasing Y_2O_3 content, with the same labels used by Erbe and Day,[6] which differ from those used in our previous work.[13]

Models of the YAS compositions in Table 1 were obtained using classical molecular dynamics (MD) simulations with the DLPOLY code.[20] The melt-and-quench simulation methodology and the interatomic potential were identical to those used in our previous work,[13] which produced structural features in agreement with ab initio results[21] and with the available experimental data on YAS[22−24] and related glasses.[25−27]

In particular, the interatomic potential is a pairwise Buckingham potential with the form

$$V_{ij}(r) = \frac{q_i q_j}{4\pi\varepsilon_0 r} + A_{ij}\exp(-r/\rho_{ij}) - C_{ij}/r^6 \quad (1)$$

where $V_{ij}(r)$ is the potential energy between two atoms of species i and j separated by r, q_i is the charge of atom i, and A_{ij}, ρ_{ij}, and C_{ij} are the potential parameters reported in Table 2, which have previously proven adequate to model a range of amorphous silicate oxides containing various amounts of other ions, including yttrium and aluminum.[25,28−30]

The experimental densities of these compositions are essentially linearly dependent on the yttria content,[31] so the simulated densities (Table 1) were chosen to reproduce this

Table 2. Buckingham Potential Parameters Used

pairs	A (eV)	ρ (Å)	C (eV Å^6)
$O^{-1.2}$–$O^{-1.2}$	2029.2204	0.343645	192.28
$Si^{+2.4}$–$O^{-1.2}$	13702.9050	0.193817	54.681
$Al^{+1.8}$–$O^{-1.2}$	12201.417	0.195628	31.997
$Y^{+1.8}$–$O^{-1.2}$	29526.977	0.211377	50.477

dependence, as well as be consistent with the densities used previously.[13] Each model included about 2000 atoms, enclosed in a periodic cubic cell of ∼30 Å, reproducing the room-temperature densities reported in Table 1. We followed a well-established general methodology to generate models of melt-derived bulk glasses through MD simulations.[9,15,25,32,33] Initially, all atoms were placed randomly in the cell, subject to the constraint that no two atoms can approach within 80−90% of their expected separation, in order to prevent unphysical starting positions. The models were then equilibrated at constant volume (NVT ensemble) for 200 ps at 6000 K, before cooling them to room temperature (300 K) at a quench rate of 1 K/ps. At 300 K, they were further equilibrated in the NVT ensemble for 200 ps, before a final 400 ps production run in the same ensemble. Throughout, the MD time step used was 2 fs, and the short-range forces were truncated at 8 Å. The Ewald summation was used to evaluate the electrostatic forces, with a real-space cutoff of 12 Å. All data given are averaged over configurations taken from these production runs at 300 K.

Once we had obtained reliable models of all the glass compositions, various structural parameters were directly calculated from the room-temperature MD trajectories, and different combinations of these parameters were investigated in order to find the combination that could best describe the trend in the experimental solubility, based on the corresponding fit.

RESULTS

New Compositions. The bulk structures of the present YAS glass compositions have similar features to those previously studied,[13] which are briefly summarized here.

The structure of YAS glass comprises a disordered connected aluminosilicate glass network, with yttrium acting as a modifier atom, breaking T−O−T bonds (T = Si or Al), causing the formation of nonbridging oxygen atoms and disrupting the glass network;[13,21−24,28,34] an example is shown in Figure 1. We find that silicon is always four-coordinated but that the average aluminum coordination number varies from 4.0 to 4.3 (reflecting the presence of both four- and five-coordinated species) and increases with increasing yttria content. Typical bond lengths are 1.6 Å for Si−O and 1.8 Å for Al−O. The network-modifying cation, yttrium, has a coordination number ranging from 6.2 to 6.8, broadly increasing with increasing yttria content. The Y−O bond length is typically 2.3 Å for these compositions. These features were in general agreement with experimental data on the structure of these and related silicate glasses.[22−27,34]

Structural Descriptor. The main task of this work is to identify structural parameters that would correlate well with the solubility of the system, based on previous findings and chemical intuition.

The first possibility to consider obviously involves predicting the solubility of a glass directly from its composition. We know that, in YAS glass, yttrium acts as a modifier atom, causing the formation of nonbridging oxygen atoms and disrupting the

dx.doi.org/10.1021/jp304200f | J. Phys. Chem. B 2012, 116, 12614−12620

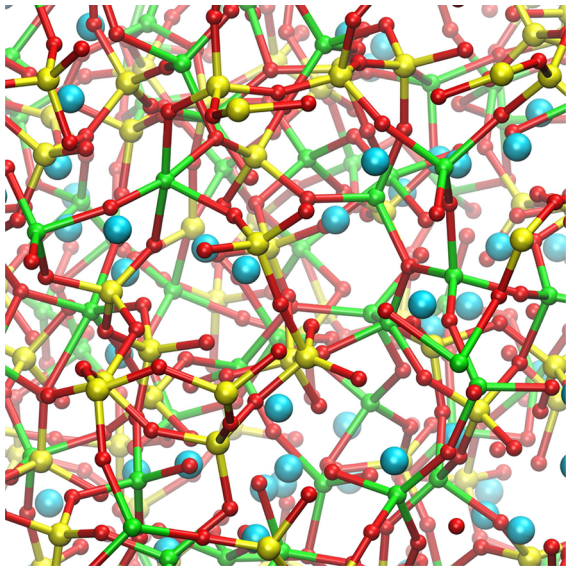

Figure 1. Snapshot of part of one of the models of the YAS-3 composition. The aluminosilicate network is shown as balls and sticks, with silicon atoms in yellow, aluminum atoms in green, and oxygen atoms in red. The network-modifying yttrium atoms are shown in cyan.

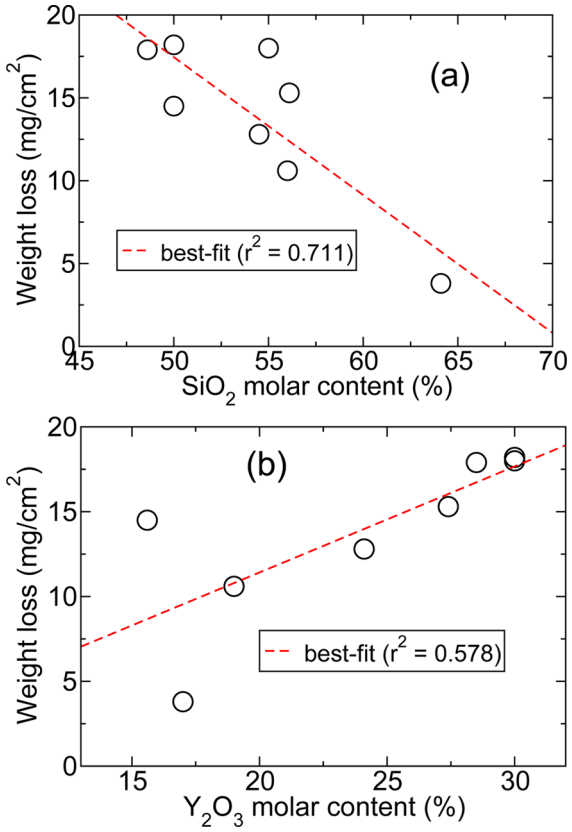

Figure 2. Best-fit linear dependences of (a) SiO_2 molar content (r^2 = 0.711, σ = 2.46 mg/cm^2) and (b) Y_2O_3 molar content (r^2 = 0.578, σ = 2.97 mg/cm^2) with solubility.

glass network. We also know that a more fragmented network typically has lower durability[35] and will likely be more prone to dissolution in an aqueous environment. It is reasonable, therefore, to suppose that solubility might be correlated with the amount of yttria in the glass. Similarly, the glass bioactivity (which reflects its dissolution rate[36]) varies substantially with silica content; for example, for Hench-type bioglass compositions,[37] those with 45 wt % SiO_2 are bioactive, whereas those with >60 wt % SiO_2 are bioinactive.[36,38] It is thus likely that the solubility and SiO_2 content are also correlated. We found that the correlation coefficient of the linear fit of Y_2O_3 molar content versus solubility was r^2 = 0.578, whereas for SiO_2 molar content, r^2 was 0.711 (Figure 2). It is clear that neither parameter can give a particularly good fit to the solubility data. This indicates that the solubility of the glass is dependent on structural features that have a more complicated dependence on composition. We need, therefore, to turn to the detailed structural analysis available from computer simulation.

The network connectivity (NC) is a structural feature well correlated with bioactivity.[15] Indeed, an empirical limit of NC ~ 3 is sometimes used to divide bioactive (NC < 3) from bioinactive (NC > 3) compositions.[15] In YAS glass, we have two network formers: silicon and aluminum. Therefore, we define a bridging oxygen (BO) atom as one that bridges two (or more) silicon or aluminum atoms, as they both form part of the connected aluminosilicate glass network. For each composition, we then computed the network connectivity of the silicon atoms alone, the aluminum atoms alone, and both species combined, that is, the average number of BO atoms coordinated to a silicon atom, an aluminum atom, or both. The r^2 parameter for these network connectivities also denoted poor correlation with the solubility. They were r^2 = 0.472 for NC(Si) (σ = 3.33 mg/cm^2),[39] r^2 = 0.375 for NC(Al) (σ = 3.62 mg/cm^2), and r^2 = 0.377 (σ = 3.61 mg/cm^2) for the total NC(Si + Al). This implies that neither the network connectivity alone is sufficient to predict changes in the glass solubility.

When considering fluoro-phosphosilicate glasses, Lusvardi et al.[16] derived a structural descriptor of their glass structures that estimated the overall strength of the network and correlated very well (r^2 = 0.912) with the glass transition temperature and with the amount of the glass leached into solution (r^2 = 0.965). This parameter explicitly takes into account the different effects of the oxygen and fluorine anions in their compositions. This same parameter can be computed for the YAS systems as well, but in this case, it does not correlate well with the solubility, with an r^2 value of 0.477 (σ = 3.31 mg/cm^2). This parameter may be more suitable for capturing bulk structure−dissolution effects in systems with multiple anions; among their results, Lusvardi et al.[16] note that considering only the oxygen atoms led to a similarly poor correlation.

To take into account more effectively the connectivity of the silicon atoms in the network, we introduced a new parameter CN_{SiOSi}, illustrated in Figure 3. The central silicon atom in the figure is four-coordinated; three of its neighbors are bridging oxygen atoms (O_1, O_2, and O_4), making the central Si a Q^3 species. The total threefold connectivity of this atom can be split into Si−O−Si and Si−O−Al connectivities of two and one, respectively. Rather than these "standard" connectivities, we considered a new parameter CN_{SiOSi}, which is the average O−Si coordination number of oxygen atoms already coordinated to at least another silicon atom (not counted in CN_{SiOSi}). Hence, among the O atoms bonded to the central Si in the figure, O_1 and O_2 have CN_{SiOSi} = 1, and O_3 and O_4 have CN_{SiOSi} = 0, for an average of 0.5.

The r^2 parameter for the correlation between CN_{SiOSi} and the solubility was 0.909 (σ = 1.38 mg/cm^2), which represents the

dx.doi.org/10.1021/jp304200f | J. Phys. Chem. B 2012, 116, 12614−12620

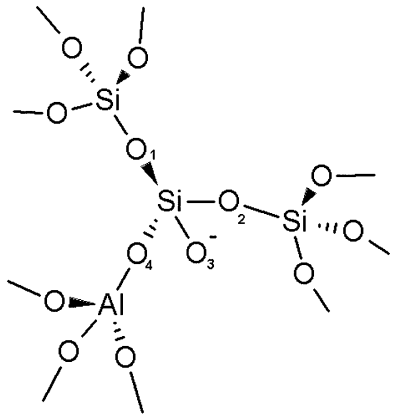

Figure 3. A silicon atom and its neighbors, with an average CN_{SiOSi} = 0.5.

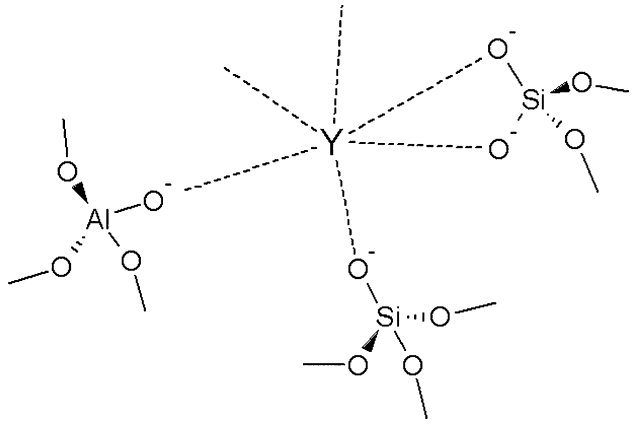

Figure 4. Examples of intertetrahedral (left and bottom) and intratetrahedral (right) coordination to the central yttrium.

best single-parameter correlation found here. We then considered additional structural factors that could be combined with the (Si−)O−Si coordination number to improve the fitting further.

Ion aggregation in clusters affects bioactivity[11,15] and is also observed in certain compositions of YAS glass.[13] We computed the yttrium clustering ratio R_{YY} using the ratio of the measured Y−Y coordination number (at a cutoff of 5 Å) to the number expected if the yttrium atoms were distributed uniformly (randomly) throughout the available space.[13,14] R_{YY} values are given in Table 3 for each composition. Values of $R_{YY} > 1$ denote spatial clustering, while $R_{YY} = 1$ describes a uniform distribution of Y atoms throughout the available space.

Table 3. Compositions and the Structural Parameters That Make Up the Descriptor *s* for All YAS Glass Compositions Considered

composition	CN_{SiOSi}	R_{YY}	N_{intra}	*s*
YAS-10	0.268	1.163	0.144	0.152
YAS-4	0.498	1.220	0.130	0.229
YAS-6	0.348	1.125	0.196	0.167
YAS-3	0.278	1.094	0.205	0.141
YAS-9	0.302	1.058	0.238	0.142
YAS-2	0.205	1.053	0.190	0.118
YAS-11	0.264	1.049	0.269	0.125
YAS-12	0.191	1.164	0.251	0.114

We also considered the number of intratetrahedral Y−O links per yttrium atom, N_{intra}. Examples of inter- and intratetrahedral bonding are given in Figure 4, in which an yttrium atom and four of its coordinated oxygen neighbors are shown. The two oxygen neighbors at the left and at the bottom are intertetrahedrally linked to the central Y; that is, they are the only oxygen atoms in their TO_x (T = Si or Al) polyhedron coordinated to yttrium. On the other hand, the two oxygen atoms coordinated to Y on the right belong to the same tetrahedron and are hence an example of intratetrahedral bonding. The potential correlation of this parameter with the glass durability can be understood as follows: if all of the approximately six oxygen neighbors in yttrium's first coordination shell come from different SiO_x or AlO_x polyhedra, then the yttrium atom is essentially connecting and to some extent contributing to the cohesion of about six different fragments of the aluminosilicate glass network. On the other hand, if some of its oxygen neighbors belong to the same TO_x polyhedron, then the resulting intratetrahedral $O_xTO_2\cdots Y$ links reduce the number of separate individual fragments associated with the same yttrium atom. In general, any increase in the amount of intratetrahedral Y−O coordination will decrease the number of fragments of the glass network coordinated to yttrium. Because the strong Y−O interaction can be expected to reduce the mobility and increase the resistance to dissolution of these fragments, a positive correlation between the extent of intratetrahedral Y−O coordination and glass solubility can also be expected.

As shown in Figure 4, intratetrahedral bonding can occur via either a silicon or an aluminum atom. We have seen that the (modified) silicate connectivity CN_{SiOSi} is strongly correlated to the solubility, whereas the aluminum network seems to have a less important role. We computed the number of intratetrahedral bonds per yttrium atom via silicon and aluminum atoms separately, as well as via both network formers. When combined with the CN_{SiOSi} connectivity and Y−Y clustering ratio, we found that the best descriptor incorporated the intratetrahedral bonding via silicon atoms alone. The number N_{intra} of intratetrahedral O−Si−O bonds per yttrium atom for the various YAS glass compositions is given in Table 3.

We combined these three features in a structural descriptor *s*

$$s = \alpha[(\text{Si}-)\text{O}-\text{Si coordination number}] + \beta[\text{Y}-\text{Y clustering ratio}] + \gamma[\text{number of intratetrahedral O}-\text{Si}-\text{O bonds per Y}] \quad (2)$$

where α, β, and γ were the best-fit coefficients, leading to r^2 = 0.955 (σ = 0.97 mg/cm^2), a further substantial improvement over using the (Si−)O−Si coordination number alone. The best-fit values of the coefficients are α = 0.310, β = 0.076, and γ = −0.136. The values of *s* for each composition are given in Table 3, and their variation with weight loss is shown in Figure 5, with only a small deviation away from linear behavior.

The values reported above for the single- and three-parameter fits denote that CN_{SiOSi} captures most of the experimental trends; the observed improvements for its combinations with other parameters obviously arise, in part, from the larger number of parameters in the fit. At the same time, as shown in the Supporting Information, out of several other possibilities, the specific combination of CN_{SiOSi} with R_{YY} and N_{intra} is the one that leads to the largest r^2, indicating that,

dx.doi.org/10.1021/jp304200f | J. Phys. Chem. B 2012, 116, 12614−12620

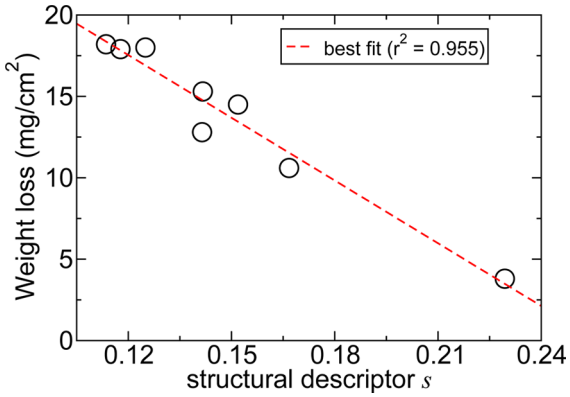

Figure 5. Weight loss as a function of the structural descriptor s, and the best-fit linear dependence.

after CN_{SiOSi}, R_{YY} and N_{intra} are the properties that carry the highest intrinsic information on the experimental solubility.

Another important issue to consider is the specific mathematical dependency of s on the three parameters identified above. A linear dependence is of course the simplest possibility, but partially nonlinear fits can, in some cases, lead to closer fits (see the Supporting Information). Of course, in principle, a higher-order polynomial or another nonlinear equation could eventually be identified, which would lead to a very close fit, but only at the expense of a significant loss in predictive power (i.e., the ability to interpolate/extrapolate outside the fitted data points). The good performances of the s descriptor thus denote that, for the present small data set, a linear fit is adequate to capture the general trend without significantly compromising the predictive power of the model.

It should be noted that the experimental error on the weight loss is ±0.1 mg/cm^2, which is much smaller than the standard deviation of even the best-fit expression for s. This means that the specific differences are mostly due to s obviously not able to capture exactly all the features that control weight loss, rather than to any experimental errors.

DISCUSSION

The target of the present simulations was to identify correlations between specific structural features and experimental solubility of YAS glasses, and to incorporate these features in a predictive model. Multivariate approaches[40] are frequently needed to reveal and interpret hidden correlations in large data sets.[41] For a small data set like the present one, however, the same goal can be reached through a simpler direct approach. By testing and comparing different possibilities, we have identified a structural descriptor s that correlates very well to the solubility, for a wide range of YAS compositions:

$$s = 0.31 \cdot CN_{SiOSi} + 0.076 \cdot R_{YY} - 0.136 \cdot N_{intra} \quad (3)$$

In the present case, the linear combination of three structural features leads to a highly representative single descriptor, suitable to draw predictive conclusions on the solubility based on structural features extracted from the models. Moreover, the limited number of parameters/variables in the fitting model allows us to understand the role and relative importance of each individual feature based on the actual values of the fitting coefficients. We see from Figure 5 that, as s increases, the solubility of the glass decreases. The coefficients of the first two terms of s are positive, implying that increasing the (Si−)O−Si coordination number and/or increasing the Y−Y clustering ratio will lead to decreasing solubility. Conversely, the sign of the third term of s is negative, implying that an increase in the number of intratetrahedral O−Si−O bonds around the yttrium atoms will increase the solubility.

The signs of the first two terms are straightforward to interpret. Although the (Si−)O−Si coordination number is not directly proportional to the network connectivity, it is clear that increasing this coordination number will lead to a more connected and less fragmented glass network, and a composition that is hence likely to be more durable. Likewise, we know from other systems[15] that an increase in modifier cation clustering is likely to enhance durability and reduce solubility. The sign of the third term (N_{intra}) can be understood as follows. We have recently shown[14,19] that the tendency of a modifier cation M to coordinate oxygen atoms bonded to the same network former (intratetrahedral M−O coordination) or to different network formers (intertetrahedral M−O coordination) depends on the physicochemical properties of the modifier cation itself. Yttrium atoms show a marked preference for intertetrahedral coordination, compared to lower-valence cations. Intertetrahedral coordination by a single modifier may increase the strength (and the durability in a physiological environment) of the network by binding together separate fragments of the glass network. On the other hand, intratetrahedral coordination may be expected to indirectly have the opposite effect: the larger the intratetrahedral component within the coordination shell of a given Y, the smaller the intertetrahedral cohesion produced by that Y. A higher N_{intra} should then lead to higher solubility, hence the negative sign of its coefficient in eq 3. Even though it has a significant impact already for YAS glasses, the N_{intra} parameter of the structural descriptor probably will find greater application in systems with more than one modifier atom, where we have recently observed[14] different amounts of intratetrahedral bonding around different modifier ions.

This work shows that the solubility of a glass is not a simple function of its composition. The structural descriptor we have devised, which does correlate very well with solubility, cannot be derived as a straightforward function of the composition. To elucidate the various structural factors that make YAS glass suitable for radiotherapy, and to optimize its properties for that application, our approach involves MD simulations to extract the atomistic properties needed to build the structural descriptor s. Figure 5 shows that, in order to minimize solubility, one should target a high value of s. On the basis of its dependence on the structural parameters discussed above, a high s value implies high silicon−silicon connectivity, large amounts of yttrium clustering, and small amounts of intratetrahedral O−Si−O bonding around yttrium. Silicon−silicon connectivity typically increases with increasing silica content (Table 3) and decreases with increasing yttria content, as the yttrium atoms break up the Si−O−Si connections. Although the dependence is not monotonic, yttrium−yttrium clustering is typically stronger at low yttria content (Table 3). These two features, therefore, point toward low-yttria- and high-silica-content YAS glass as most suitable for radiotherapy, in accordance with the current use of the YAS-4 composition in clinical applications.

The term involving the number of intratetrahedral O−Si−O bonds per yttrium atom is rather smaller, on average about one-third of the magnitude of either of the other two terms. It is also difficult to understand which features control the amount of such intratetrahedral bonding, which varies by a factor of 2

across these compositions (Table 3). Very roughly, inspecting Table 3 shows that increasing yttria content increases the amount of intratetrahedral bonding, which would imply again that low-yttria-content glasses are most suitable.

It is more difficult to understand the role of aluminum in these glasses and the effect of changing the alumina content. Although both aluminum and silicon form part of the disordered glass network, the present results suggest that it is the silicate part of the network that is of more relevance to the solubility; we have seen that Al_2O_3 content does not correlate well with solubility, nor do network connectivities that involve aluminum, and intratetrahedral bonding involving aluminum correlates less well with solubility than that involving silicon. Our analysis points out that a representative description of structure−solubility relations can be obtained without including aluminum-specific parameters. This extends the applicability of the new structural descriptor to Al-free glasses.

The above considerations suggest that the optimal glass for radiotherapy would have a high silica and a low yttria content. However, the yttria content cannot be lowered too far because then the amount of radiation incident on the tumor would be too low for an effective treatment. Also, glasses containing low concentrations of yttrium require long times, usually several weeks,[42] to activate the radioisotopes through neutron bombardment before the therapy can begin, which could represent an unacceptable delay in the treatment.

The optimal strategy, therefore, would be to use clinical considerations to understand the minimum yttria content needed for a successful treatment, and synthesize a high-silica glass composition with this amount of yttria, ensuring that the silica content is high enough that, even after yttrium inclusion, the silicon−silicon connectivity in this glass (the single parameter with the strongest impact on the solubility) remains sufficiently high.

CONCLUSIONS

The dissolution behavior of yttrium silicate glasses critically affects their suitability as radioisotope carriers in radiotherapy. In this work, we have identified specific structural features of the glasses that can be extracted from MD simulations and used to predict the solubility of these materials through a structural descriptor, also devised in this work.

To identify the structural factors that control the solubility of yttrium aluminosilicate glasses, we have carried out classical molecular dynamics simulations of eight different compositions, the solubilities of which have previously been measured experimentally. We have found that simple parameters, such as silica or yttria content or standard network connectivity, are not suitable to explain the observed dependence of solubility on the glass composition. We thus considered further structural features with a potential correlation to the dissolution behavior and identified their best combination. In particular, a linear combination of (Si−)O−Si coordination number, Y−Y clustering ratio, and number of intratetrahedral O−Si−O bonds per Y shows a high correlation with the experimental solubility.

To be used in in situ radiotherapy, a YAS glass is required to have high durability (low solubility), which corresponds to larger values of the *s* descriptor. The latter incorporates the complex connections between composition, structure, and durability of YAS glasses and points to the best directions to optimize these materials for in situ radiotherapy. Because it only depends on features involving the silicate network and the radioisotope (network-modifier) ions, this model should be easily extended to other aluminum-free materials with potential use in radiotherapy, such as bioactive glasses.[14]

The strong correlations found between bulk structural features and the glass solubility confirm that the bulk structure of a glass determines its dissolution behavior, which also entails that structural features detected for the bulk glass persist upon solvation. Nonetheless, an explicit investigation of the effective dissolution process of these materials would certainly be worth a future study, for instance, to identify additional features of the interface that can also play a role in the process of dissolution.[43−45]

ASSOCIATED CONTENT

Supporting Information

Performances of structural descriptors with alternative choices of parameters and mathematical dependencies. This material is available free of charge via the Internet at http://pubs.acs.org.

AUTHOR INFORMATION

Corresponding Author

*E-mail: a.tilocca@ucl.ac.uk.

Notes

The authors declare no competing financial interest.

ACKNOWLEDGMENTS

The UK's Royal Society (RS-URF) and EPSRC (Grant EP/F020066/1) are gratefully acknowledged for financial support. Computing resources were provided by the UCL Legion HPC Facility and the HECToR supercomputing service (via the EPSRC-funded Materials Chemistry Consortium).

REFERENCES

(1) Chen, S.-D.; Hsueh, J.-F.; Tsai, S.-C.; Lin, W.-Y.; Cheng, K.-Y.; Wang, S.-J. *Nucl. Med. Commun.* **2001**, *22*, 121−125.
(2) Hench, L. L.; Day, D. E.; Höland, W.; Rheinberger, V. M. *Int. J. Appl. Glass Sci.* **2010**, *1*, 104−117.
(3) Gaba, R. C.; Lewandowski, R. J.; Kulik, L. M.; Riaz, A.; Ibrahim, S. M.; Mulcahy, M. F.; Ryu, R. K.; Sato, K. T.; Gates, V.; Abecassis, M. M.; et al. *Ann. Surg. Oncol.* **2009**, *16*, 1587−1596.
(4) El-Serag, H. B.; Mason, A. C.; Key, C. *Hepatology* **2001**, *33*, 62−65.
(5) Audi, G.; Bersillon, O.; Blachot, J.; Wapstra, A. H. *Nucl. Phys. A* **2003**, *729*, 3−128.
(6) Erbe, E. M.; Day, D. E. *J. Biomed. Mater. Res.* **1993**, *27*, 1301−1308.
(7) Sarnthein, J.; Pasquarello, A.; Car, R. *Phys. Rev. Lett.* **1995**, *74*, 4682−4685.
(8) Vollmayr, K.; Kob, W.; Binder, K. *Phys. Rev. B* **1996**, *54*, 15808−15827.
(9) Tilocca, A.; de Leeuw, N. H.; Cormack, A. N. *Phys. Rev. B* **2006**, *73*, 104209.
(10) Tilocca, A. *Phys. Rev. B* **2007**, *76*, 224202.
(11) Tilocca, A. *J. Mater. Chem.* **2010**, *20*, 6848−6858.
(12) Tilocca, A.; Cormack, A. N.; de Leeuw, N. H. *Chem. Mater.* **2007**, *19*, 95−103.
(13) Christie, J. K.; Tilocca, A. *Chem. Mater.* **2010**, *22*, 3725−3734.
(14) Christie, J. K.; Malik, J.; Tilocca, A. *Phys. Chem. Chem. Phys.* **2011**, *13*, 17749−17755.
(15) Tilocca, A. *Proc. R. Soc. A* **2009**, *465*, 1003−1027.
(16) Lusvardi, G.; Malavasi, G.; Tarsitano, F.; Menabue, L.; Menziani, M. C.; Pedone, A. *J. Phys. Chem. B* **2009**, *113*, 10331−10338.
(17) Lusvardi, G.; Malavasi, G.; Menabue, L.; Menziani, M. C.; Pedone, A.; Segre, U. *J. Eur. Ceram. Soc.* **2007**, *27*, 499−504.

(18) Linati, L.; Lusvardi, G.; Malavasi, G.; Menabue, L.; Menziani, M. C.; Mustarelli, P.; Segre, U. *J. Phys. Chem. B* **2005**, *105*, 4989−4998.
(19) Christie, J. K.; Tilocca, A. *J. Mater. Chem.* **2012**, *22*, 12023−12038.
(20) Smith, W.; Forester, T. R.; Todorov, I. T. DL_POLY is a molecular dynamics simulation package that has been obtained from STFC's Daresbury Laboratory via the website http://www.ccp5.ac.uk/DL_POLY.
(21) Christie, J. K.; Tilocca, A. *Adv. Eng. Mater.* **2010**, *12*, B326−B330.
(22) Pozdnyakova, I.; Sadiki, N.; Hennet, L.; Cristiglio, V.; Bytchkov, A.; Cuello, G. J.; Coutures, J. P.; Price, D. L. *J. Non-Cryst. Solids* **2008**, *354*, 2038−2044.
(23) Florian, P.; Sadiki, N.; Massiot, D.; Coutures, J. P. *J. Phys. Chem. B* **2007**, *111*, 9747−9757.
(24) Schaller, T.; Stebbins, J. F. *J. Phys. Chem. B* **1998**, *102*, 10690−10697.
(25) Du, J.; Benmore, C. J.; Corrales, R.; Hart, R. T.; Weber, J. K. R. *J. Phys.: Condens. Matter* **2009**, *21*, 205102.
(26) Wilding, M. C.; Benmore, C. J.; McMillan, P. F. *J. Non-Cryst. Solids* **2002**, *297*, 143−155.
(27) Schmücker, M.; Schneider, H. *J. Non-Cryst. Solids* **2002**, *311*, 211−215.
(28) Du, J. *J. Am. Ceram. Soc.* **2009**, *92*, 87−95.
(29) Thomas, B. W. M.; Mead, R. N.; Mountjoy, G. *J. Phys.: Condens. Matter* **2006**, *18*, 4697−4708.
(30) Johnson, J. A.; Benmore, C. J.; Holland, D.; Du, J.; Beuneu, B.; Mekki, A. *J. Phys.: Condens. Matter* **2011**, *23*, 065404.
(31) Day, D. E.; Day, T. E. Radiotherapy Glasses. In *An Introduction to Bioceramics*; Hench, L. L., Wilson, J., Eds.; World Scientific: Singapore, 1993.
(32) Mead, R. N.; Mountjoy, G. *J. Phys. Chem. B* **2006**, *110*, 14273−14278.
(33) Lusvardi, G.; Malavasi, G.; Cortada, M.; Menabue, L.; Menziani, M. C.; Pedone, A.; Segre, U. *J. Phys. Chem. B* **2008**, *112*, 12730−12739.
(34) Marchi, J.; Morais, D. S.; Schneider, J.; Bressiani, J. C.; Bressiani, A. H. A. *J. Non-Cryst. Solids* **2005**, *351*, 863−868.
(35) Tilocca, A. *J. Chem. Phys.* **2010**, *133*, 014701.
(36) Hench, L. L. *J. Am. Ceram. Soc.* **1998**, *81*, 1705−1728.
(37) Hench, L. L. *Science* **1980**, *208*, 826−831.
(38) Fujibayashi, S.; Neo, M.; Kim, H.; Kokubo, T.; Nakamura, T. *Biomaterials* **2003**, *24*, 1349−1356.
(39) Standard deviations are calculated according to the conventional definition given in ref 40, as the square root of the averaged square difference between the observed and predicted values.
(40) Le, T.; Epa, V. C.; Burden, F. R.; Winkler, D. A. *Chem. Rev.* **2012**, *112*, 2889−2919.
(41) Duee, C.; Desanglois, F.; Lebecq, I.; Follet-Houttemane, C. *J. Non-Cryst. Solids* **2012**, *358*, 1083−1090.
(42) Yamashita, K.; Nakamura, S. *J. Ceram. Soc. Jpn.* **2005**, *11*, 1−9.
(43) Tilocca, A.; Cormack, A. N. *J. Phys. Chem. C* **2008**, *112*, 11936−11948.
(44) Tilocca, A.; Cormack, A. N. *ACS Appl. Mater. Interfaces* **2009**, *1*, 1324−1333.
(45) Tilocca, A.; Cormack, A. N. *Langmuir* **2010**, *26*, 545−551.